Indentation analysis of plasma-sprayed Cr_3C_2-NiCr coatings

J. F. LI*, X. Y. WANG‡, H. LIAO
LERMPS, Université de Technologie de Belfort-Montbéliard, 90 010 Belfort Cedex, France

C. X. DING
Shanghai Institute of Ceramics, Chinese Academy of Sciences, Shanghai 200050, People's Republic of China

C. CODDET
LERMPS, Université de Technologie de Belfort-Montbéliard, 90 010 Belfort Cedex, France

Thermal spray coatings are widely applied as antiwear solutions in a variety of industries. In such applications, the coatings are frequently susceptible to two competing mechanical responses, (a) indentation deformation and (b) fracture, caused by erodent, abrasive, and debris originated from the environment or produced during use [1–4]. Microhardness and fracture toughness can quantify the resistance to deformation and fracture, respectively [5]. Thus indentation tests, especially Vickers indentation tests for determining the microhardness and fracture toughness of materials, are commonly used as quality control tools. Correspondingly, the Vickers hardness of thermal spray coatings considering measurement locations, directions, and indenter loads were studied [6–8]. The fracture toughness values of some coatings were measured employing the Vickers indentation technique and correlated with the friction and wear behaviors of the coatings [4, 9, 10]. However, no attempt was made so far to combine the Vickers hardness and fracture toughness into a common description for thermal spray coatings.

Thermal sprayed Cr_3C_2-NiCr coatings are often used in high temperature applications such as in turbine engine and steel industry [2, 4, 11, 12]. Several studies have contributed to the processing, characterization, mechanical, and tribological properties of this type of coating [2, 4, 8, 11–18]. Plastic deformation [15], interlamellar boundary sliding [8, 17, 18], and intralamellar cracking, [19] were proposed to explain the mechanical properties and wear behavior of these coatings. In the present study, a universal deformation/fracture diagram, based on the methodology developed by Lawn and Marshall [5], has been presented for plasma-sprayed Cr_3C_2-NiCr coatings using several feedstock materials. The threshold loads and crack dimensions that the coatings might sustain in a contact event, without the onset of fracture, are obtained from the universal deformation/fracture diagram. The purpose of this paper is to assess the susceptibilities to deformation and fracture of the coatings with respect to the starting powders, coating microstructure, and indentation direction, so as to provide a physical insight into the mechanical and tribological properties of the coatings.

The Cr_3C_2-NiCr coatings were applied onto FeCr18Ni9Ti stainless steel plates using a Sulzer-Metco F4-MB gun mounted on an ABB S3 robot with different starting powders and substrate dimensions (Table I). The starting powders and plasma parameters have been described in detail in the previous papers [16, 18–20]. Prior to indentation tests, all the samples were first ground using 7–10 μm emery, and then were further polished using 1 to 0.5 μm diamond paste.

It was experimentally confirmed that the Knoop hardness measured on cross sections was in between and very close to the Vickers hardness measured on cross section and surface (sample V75T1200) at different indenter loads [8, 19]. Therefore, the Knoop indentation tests were first carried out on the cross sections of the coatings using an HX-1000 microhardness tester (Shanghai Second Optical Instrument Factory, China) at a load of 1 kgf to determine the hardness (H) and simultaneously the elastic modulus (E) of the coatings [19, 21]. For each coating, 20 indents were performed and results were averaged out to obtain hardness and elastic modulus.

The Vickers indentation tests were then performed using an Akashi Avk-A indenter to determine the indentation parameters associated with radial cracking. The radial crack lengths, $2C$, were measured with an optical microscope immediately after releasing the load. Sample V75T1200 was tested both on cross section and surface, samples V50T520 and V100T1250 were tested only on cross sections, and the other samples were tested only on surfaces. The indenter load chosen for indentation tests on the cross sections was 10 kgf, and that for indentation tests on the surfaces was 30 kgf. For each test, the measurement series comprised 10 readings, which were randomly located on the surface or the cross section and separated by a distance greater than the diameter of the radial cracks. The fracture toughness of the coatings was calculated from the following equation [9]

$$K_C = 0.016(E/H)^{1/2}(P/C)^{3/2} \quad (1)$$

where the radial crack dimension, $2C$ was obtained from the mean of the 10 readings. For the tests on the

*Present address: Laser Processing Research Centre and Corrosion and Protection Centre, UMIST, P.O. Box 88, Manchester M60 1QD, UK.
‡Present address: The Department of Textile, UMIST, P.O. Box 88, Manchester M60 1QD, UK.

0022–2461

TABLE I The Cr_3C_2-NiCr coatings chosen for indentation analysis

Code	Starting powder[a]	Substrate dimension (mm^3)	Coating thickness (μm)	Porosity[b] (%)
V75T1200	Sulzer-Metco 82VF-NS, mechanically blended Cr_3C_2-NiCr (7 wt%NiCr)	50 × 30 × 2	1200	2.6
V50T520		50 × 30 × 2	520	3.6
V100T1250		50 × 30 × 2	1250	3.2
82VF-NS		30 × 7 × 6	1000	5.4
AMDRY308	Sulzer-Metco AMDRY308, mechanically blended Cr_3C_2-NiCr (15 wt%NiCr)	30 × 7 × 6	1000	6.8
81VF-NS	Sulzer-Metco 81VF-NS, mechanically blended Cr_3C_2-NiCr (15 wt%NiCr)	30 × 7 × 6	1000	4.9
SHANGNAI	Pre-sintered Cr_3C_2-NiCr (25 wt%NiCr)	30 × 7 × 6	1000	8.8
CRC15NI	Ni-clad Cr_3C_2 (15 wt%Ni)	30 × 7 × 6	1000	2.8
CRC20NI	Ni-clad Cr_3C_2 (20 wt%Ni)	30 × 7 × 6	1000	2.9
CRC25NI	Ni-clad Cr_3C_2 (25 wt%Ni)	30 × 7 × 6	1000	3.8

[a]Except for the commercially available Sulzer-Metco powders, the other powders were prepared by the authors [18, 20].
[b]Porosity values were measured using the microscopic count method [16].

cross sections, K_C was calculated as $K_{C,CSP}$ and $K_{C,CSV}$ respectively from the radial cracks parallel to and perpendicular to the interlamellar boundary direction, i.e., C_{CSP} and C_{CSV} (Fig. 1). Considering the directions of crack propagation and strain stress at the crack tip, the elastic moduli measured using the Knoop indentation tests on the cross sections were adopted to calculate $K_{C,SUR}$ and $K_{C,CSV}$, and those performed on the surfaces to calculate $K_{C,CSP}$.

Fig. 2 presents the universal deformation/fracture diagram of the various Cr_3C_2-NiCr coatings, drawn according to the procedure developed by Lawn and Marshall [5]. Here, a deformation zone is described

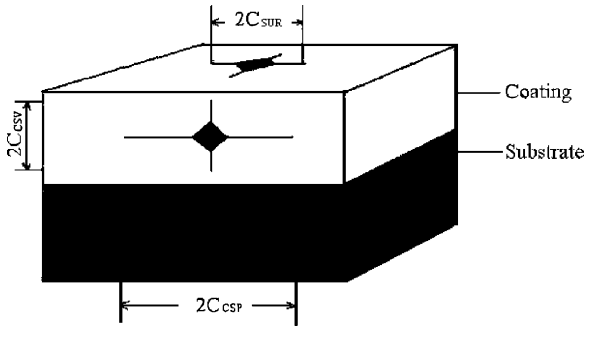

Figure 1 Schematic representation of sharp indentation induced crack patterns in the coatings.

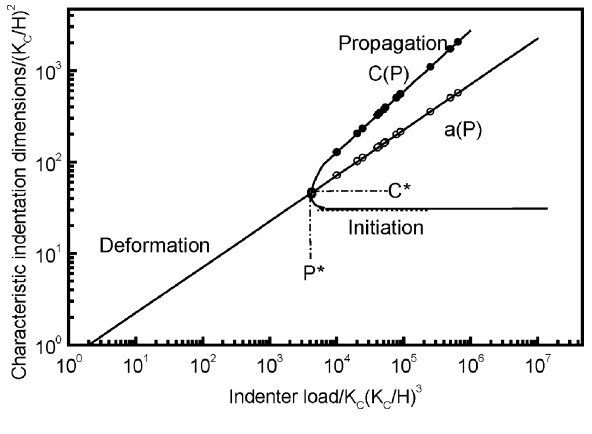

Figure 2 Universal deformation/fracture diagram of plasma sprayed Cr_3C_2-NiCr coatings.

by

$$P/a^2 = \alpha_0 H \tag{2}$$

where α_0 is an indenter constant, for the characteristic dimensions of imprint, a, and crack, C, versus load P. The fracture can be separated into the initiation and propagation stages. At the propagation stage, well-developed median cracks extend to penny-like geometry under near center-loading conditions and accordingly satisfy the following equation

$$P/C^{3/2} = \beta_0 K_C \tag{3}$$

where β_0 is another constant. It should be pointed out that this universal deformation/fracture diagram was developed for reasonably homogenous materials. Fig. 2 implies that all the fully developed median/radical cracks of $2C_{CSP}$, $2C_{CSV}$ and $2C_{SUR}$ attained the half-penny configuration in spite of the highly anisotropic behavior of the coatings, which originates from the typical lamellar structure of thermally sprayed coatings [21]. From Fig. 2, the geometrical constants of $\lambda_0 = 4.2 \times 10^3$ and $\mu_0 = 46$ are obtained from a minimum load P^* that crack initiation occurs, according to:

$$P^* = \lambda_0 K_C (K_C/H)^3 \tag{4a}$$

$$C^* = \mu_0 (K_C/H)^2 \tag{4b}$$

When compared with $\lambda_0 = 1.6 \times 10^4$ and $\mu_0 = 120$ reported by Lawn and Marshall [5] for bulk materials and $\lambda_0 = 2.2 \times 10^4$ and $\mu_0 = 44$ given by calculations based on an ideal half-penny shape median/radial crack nuclei [22], the present λ_0 value appears significantly lower. According to Equation 4a, this result demonstrates that the threshold loads that the coatings might sustain in a contact event without the onset of fracture are lower than those of the corresponding bulk materials with identical H and K_C values. This is probably related to a number of defects, such as pores, interlamellar boundaries, and intralamellar cracks [19, 21] existing in the coatings, and which may act as origins of crack nucleation. Substituting the obtained λ_0 and μ_0

TABLE II Deformation/fracture parameters and threshold parameters of median crack development

Code	Crack direction	Deformation/fracture parameter				Threshold parameter	
		H[a] (GPa)	E (GPa)	K_C (MPa$\sqrt{m}$)	H/K_C ($\mu m^{-1/2}$)	P^* (N)	C^* (μm)
V75T1200	CSP	8.5 (8.4)	110.6	3.3	2.5	0.8	7
	CSV	8.5 (8.4)	126.8	6.1	1.4	9.4	24
	SUR	8.5 (8.7)	126.8	6.9	1.2	15.8	31
V50T520	CSP	7.4	100.4	2.3	3.2	0.3	5
	CSV	7.4	115.1	5.6	1.3	10.2	26
V100T1250	CSP	7.7	91.7	2.4	3.2	0.3	4
	CSV	7.7	105.1	5.4	1.4	7.6	22
82VF-NS	SUR	7.1	85.8	6.1	1.2	15.9	34
AMDRY308	SUR	5.8	81.0	5.8	1.0	24.3	46
81VF-NS	SUR	5.9	106.7	6.2	0.9	30.1	51
SHANGNAI	SUR	6.0	86.0	5.2	1.2	13.7	33
CRC15NI	SUR	6.1	169.6	8.4	0.7	50.3	58
CRC20NI	SUR	6.0	273.3	8.7	0.7	60.5	65
CRC25NI	SUR	5.5	266.1	9.8	0.6	122.9	96

[a]The values in the parentheses are the corresponding Vickers hardness.

in Equations 4, the threshold parameters, loads P^*, in the range of 0.3 to 122.9 N, and crack lengths C^*, from 5 to 96 μm, for the different coatings were calculated and listed in Table II.

Highly anisotropic behavior of the coatings is clearly shown by the variation in the threshold loads P^* and crack lengths C^*, i.e., much lower P^* and CP^* are observed for cracks parallel to the interlamellar boundaries direction than those perpendicular to them. The former cracks actually initiate and extend along the interlamellar boundaries of the coatings, which result in interlamellar boundaries opening. Their threshold loads P^* are lower than 1 N and the threshold crack lengths C^* are smaller than 10 μm for all three tested coatings. The latter is intralamellar cracking. Thus, the interlamellar boundaries opening occurs much more easily than the intralamellar cracking.

Previous studies concerning the Cr_3C_2-NiCr coatings exhibited that the Vickers hardness decreased with increasing indenter loads [7, 8], and flake off of lamellae occurred during sliding due to intensive adhesion [17]. These results can now be explained in terms of interlamellar boundaries opening, whose threshold load and crack are rather low. For the Vickers hardness testing, the interlamellar boundaries opening commonly took place and increased with the increase in the indenter load, which led to the fact that the elastic recovery of indentation after loading was relatively reduced, and hence that the Vickers hardness decreased with increasing loads. For a sliding contact, interlamellar boundaries opening would also occur because the adhesive force would lead to a stress perpendicular to the boundary direction; boundaries opening would then occur and result in flake-off of lamellae.

Cracks C_{SUR} are also intralamellar cracking. When trying to correlate the threshold parameters of cracks C_{SUR} with starting powders (Tables I and II), one can find that the coatings deposited using the Ni-clad Cr_3C_2apparently have higher threshold loads P^* and crack lengths C^*, indicating that these coatings can sustain larger deformations without fracturing than the others. For the coatings issued from the three commercially available powders and those issued from the Ni-clad Cr_3C_2 powders, it is observed that P^* and C^* increase with increasing NiCr (or Ni) content in the powder.

Fig. 3 shows the SEM micrographs of some coating cross sections. Clearly, nickel is more homogeneously distributed in the CRC25NI coating than in the other coatings. However, it is difficult to quantitatively compare the amount of wider interlamellar boundaries and interlamellar cracks among the coatings. Combining the results shown in Fig. 3 and Table II, it can be seen that the SHANGNAI coating has more pores and hence lower threshold load P^* and crack length C^* than the other coatings. However, P^* and C^* seem out of proportion with the porosities of the coatings. For example, sample AMDRY308 has larger porosity than sample 82VF-NS, but its P^* and C^* are higher. Except for SHANGNAI coating, the more homogeneously the NiCr alloy (or Ni) is distributed in the coatings, the larger the threshold loads P^* and crack lengths C^* are. Therefore, P^* and C^* appear to be mainly related to NiCr (or Ni) content and distribution and secondarily to the porosities of the coatings.

Therefore, it can be concluded that the threshold loads of the coatings were significantly lower than those of the corresponding bulk materials considering identical hardness and fracture toughness. The threshold loads were in the range of 0.3 and 122.9 N, while the threshold crack lengths varied from 5 to 96 μm for the different coatings and testing directions. Highly anisotropic behavior of the coatings is clearly shown by the threshold parameters, with much lower threshold loads and crack lengths for cracks parallel to the surface than those for cracks perpendicular to it. The former threshold loads were lower than 1 N and threshold crack lengths were smaller than 10 μm for all tested coating samples. These threshold loads and crack lengths were mainly related to NiCr (or Ni) contents and distributions and with less extent to the porosities of coatings. A homogeneously distributed nickel chromium alloy (or nickel) matrix in the coatings clearly improved their threshold parameters.

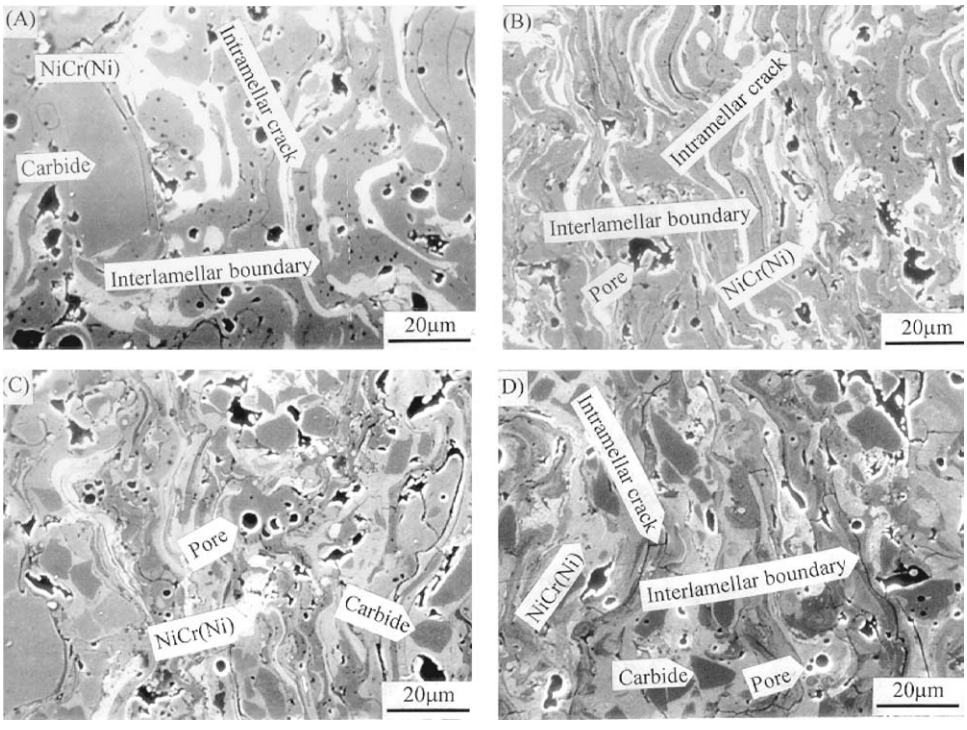

Figure 3 SEM micrographs of some coating cross sections: (A) AMDRY308, (B) 81VF-NS, (C) SHANGNAI, and (D) CRC25NI.

References

1. R. W. SMITH and R. NOVAK, *Powder Metall. Int.* **3** (1991) 147.
2. G. BARBEZAT, A. R. NICOLL and A. SICKINGER, *Wear* **162–164** (1993) 529.
3. B. Q. WANG and K. LUER, *ibid.* **174** (1994) 177.
4. G. BARBEZAT, A. R. NICOLL, Y. S. YIN and X. Y. SHENG, *Tribol. Trans.* **38** (1995) 845.
5. B. R. LAWN and D. B. MARSHALL, *J. Amer. Ceram. Soc.* **62**(7/8) (1979) 347.
6. C. C. BERNDT, J. KARTHIKEYAN, R. RATNARAJ and Y. D. JUN, in "Thermal Spray Coatings: Properties, Processes and Applications," edited by T. F. Bernecki (ASM International, Materials Park, Ohio, USA, 1992) p. 199.
7. C. K. LIN, S. H. LEIGH and C. C. BERNDT, in "Thermal Spraying: Current Status and Future Trends," edited by A. Ohmori (High Temperature Society of Japan, Osaka, Japan, 1995) p. 903.
8. J. F. LI and C. X. DING, *J. Chin. Ceram. Soc.* **28**(3) (2000) 223.
9. G. K. BESHISH, C. W. FLOREY, F. J. WORZALA and W. J. LENLING, *J. Therm. Spray Techn.* **2**(1) (1993) 35.
10. J. LI, Y. ZHANG, J. HUANG and C. DING, *ibid.* **7**(2) (1998) 242.
11. J. TAKEUCHI, Y. MURATA, Y. HARADA, T. TOMITA, S. NAKAHAMA and T. GO, in "Thermal Spray: Meeting the Challenges of the 21th Century," edited by C. Coddet (ASM International, Materials Park, Ohio, USA, 1998) p. 1425.
12. D. R. SIELSKI and P. SAHOO, in "Thermal Spray: Practical Solutions for Engineering Problems," edited by C. C. Berndt (ASM International, Materials Park, Ohio, USA, 1996) p. 159.
13. M. MOHANY, R. W. SMITH, M. DE BONTE, J. P. CELIS and E. LUGSCHEIDER, *Wear* **198** (1996) 151.
14. J. M. GUILEMANY, J. NUTTING and N. LIORCA-ISERN, *J. Therm. Spray Technol.* **5**(4) (1996) 483.
15. J. F. LI, C. X. DING, J. Q. HUANG and P. Y. ZHANG, *Wear* **211** (1997) 177.
16. J. F. LI and C. X. DING, *J. Mater. Sci. Lett.* **18** (1999) 1591.
17. *Idem.*, *Wear* **240** (2000) 180.
18. *Idem.*, *Surf. Coat. Technol.* **130** (2000) 15.
19. *Idem.*, *ibid.* **135** (2001) 229.
20. J. F. LI and C. X. DING, *Thin Solid Films* **376** (2000) 179.
21. S. H. LEIGH, C. K. LIN and C. C. BERNDT, *J. Amer. Ceram. Soc.* **80**(8) (1997) 2093.
22. B. R. LAWN and A. G. EVANS, *J. Mater. Sci.* **12**(11) (1977) 2195.
23. B. R. LAWN, A. G. EVANS and D. B. MARSHALL, *ibid.* **63**(9/10) (1980) 574.

Received 3 May
and accepted 23 June 2004